

Stringent Tests of Constrained Minimal Flavour Violation through $\Delta F = 2$ Transitions

Andrzej J. Buras and Jennifer Girrbach

TUM-IAS, Lichtenbergstr. 2a, D-85748 Garching, Germany
Physik Department, TUM, D-85748 Garching, Germany

Abstract

New Physics contributions to $\Delta F = 2$ transitions in the simplest extensions of the Standard Model (SM), the models with constrained Minimal Flavour Violation (CMFV), are parametrized by a single variable $S(v)$, the value of the real box diagram function that in CMFV is bounded from below by its SM value $S_0(x_t)$. With already very precise experimental values of ε_K , ΔM_d , ΔM_s and precise values of the CP-asymmetry $S_{\psi K_S}$ and of \hat{B}_K entering the evaluation of ε_K , the future of CMFV in the $\Delta F = 2$ sector depends crucially on the values of $|V_{cb}|$, $|V_{ub}|$, γ , $F_{B_s}\sqrt{\hat{B}_{B_s}}$ and $F_{B_d}\sqrt{\hat{B}_{B_d}}$. The ratio ξ of the latter two non-perturbative parameters, already rather precisely determined from lattice calculations, allows then together with $\Delta M_s/\Delta M_d$ and $S_{\psi K_S}$ to determine the range of the angle γ in the unitarity triangle independently of the value of $S(v)$. Imposing in addition the constraints from $|\varepsilon_K|$ and ΔM_d allows to determine the favorite CMFV values of $|V_{cb}|$, $|V_{ub}|$, $F_{B_s}\sqrt{\hat{B}_{B_s}}$ and $F_{B_d}\sqrt{\hat{B}_{B_d}}$ as functions of $S(v)$ and γ . The $|V_{cb}|^4$ dependence of ε_K allows to determine $|V_{cb}|$ for a given $S(v)$ and γ with a higher precision than it is presently possible using tree-level decays. The same applies to $|V_{ub}|$, $|V_{td}|$ and $|V_{ts}|$ that are automatically determined as functions of $S(v)$ and γ . We derive correlations between $F_{B_s}\sqrt{\hat{B}_{B_s}}$ and $F_{B_d}\sqrt{\hat{B}_{B_d}}$, $|V_{cb}|$, $|V_{ub}|$ and γ that should be tested in the coming years. Typically $F_{B_s}\sqrt{\hat{B}_{B_s}}$ and $F_{B_d}\sqrt{\hat{B}_{B_d}}$ have to be significantly lower than their present lattice values, while $|V_{cb}|$ has to be significantly higher than its tree-level determination. The region in the space of these three parameters allowed by CMFV indicates visible problems in this class of models and hints for the presence of new sources of flavour violation and/or new local operators in $\Delta F = 2$ data that are strongly suppressed in these models. As a byproduct we propose to reduce the present uncertainty in the charm contribution to ε_K by using the experimental value of ΔM_K .

1 Introduction

The simplest class of extensions of the Standard Model (SM) are models with constrained MFV (CMFV) [1–3] that similarly to the SM imply stringent correlations between observables in K , B_d and B_s systems, while allowing still for significant departures from SM expectations. In the case of $\Delta F = 2$ transitions in the down-quark sector, that is $K^0 - \bar{K}^0$ and $B_{s,d}^0 - \bar{B}_{s,d}^0$ mixings, new physics (NP) in these models enters only through a single universal real one-loop function, the box diagram function $S(v)$, with v standing for the parameters of a given CMFV model. Moreover it can be shown that in this class of models $S(v)$ is bounded from below by its SM value [4]:

$$S(v) \geq S_0(x_t) \approx 2.3 \quad (1)$$

with $S_0(x_t)$ given in (9).

It is known that the SM experiences some tension in the correlation $S_{\psi K_S} - \varepsilon_K$ [5–9]. This tension can be naturally removed in models with CMFV by enhancing the value of $S(v)$. However, as pointed out in [10, 11] this spoils the agreement of the SM with the data on $\Delta M_{s,d}$ signaling the tension between $\Delta M_{s,d}$ and ε_K in CMFV models.

Now the experimental data on ε_K , ΔM_d , ΔM_s are already very precise. Moreover the CP-asymmetry $S_{\psi K_S}$ is also measured within the accuracy of a few percent. In all CMFV models we have

$$S_{\psi K_S} = \sin 2\beta \quad (\text{CMFV}), \quad (2)$$

and consequently this implies a universal precise value of the angle β in the unitarity triangle in this class of models [1].

With $|V_{us}|$ determined already very precisely the size of the tensions mentioned above depends primary on the values of

$$|V_{cb}|, \quad F_{B_s} \sqrt{\hat{B}_{B_s}}, \quad F_{B_d} \sqrt{\hat{B}_{B_d}}, \quad \hat{B}_K, \quad \gamma, \quad S(v), \quad (3)$$

with $|V_{ub}|$ being then a derived quantity from the unitarity of the CKM matrix. The present status of these quantities can be found in Table 1. In the case of $B_{s,d}$ mesons we refer also to [12, 13].

Now the lattice QCD calculations made an impressive progress in the determination of \hat{B}_K which enters the evaluation of ε_K [14–19]. The most recent world average $\hat{B}_K = 0.767 \pm 0.010$ [20] is very close to its large N value $\hat{B}_K = 0.75$ [21, 22]. Moreover the analyses in [23] and in particular in [24] show that \hat{B}_K cannot be larger than its large N value. Therefore we expect that the final lattice value of \hat{B}_K will be slightly lower than the present one. However, as the lattice precision is already very high, we expect that the final result will be very close to 0.75 and it is a very good approximation to set simply

$$\hat{B}_K = 0.75. \quad (4)$$

Indeed compared to the present uncertainty from $|V_{cb}|$ in ε_K proceeding in this manner is fully justified.

We are then left with five variables in (3) and we can ask the question which values of them would allow to fit all $\Delta F = 2$ data within the SM and CMFV models. While such an exercise is against the spirit that γ and $|V_{cb}|$ should be determined from tree-level decays, while $F_{B_s}\sqrt{\hat{B}_{B_s}}$ and $F_{B_d}\sqrt{\hat{B}_{B_d}}$ from lattice calculations independently of NP contributions, in a concrete framework like the SM and CMFV such an exercise makes sense. In fact the determinations of some of the non-perturbative parameters from FCNC data was already performed within the SM with different goals in the analyses of the UTfit collaboration [25]. See also [9].

The spirit of the present paper differs also from our recent studies of NP models, in particular in [11, 26–31], where the emphasize has been put on correlations between observables, still to be measured, rather than the correlations between parameters of a given NP model. However, due to the shutdown of the LHC for two years not much progress in testing these correlations is expected soon. On the other hand the coming years can be considered as lattice precision era, which will allow to study NP with high precision through $\Delta F = 2$ observables for which the data are already very precise. In the field of FCNC processes this is a unique situation until now.

In order to reach our goal we need still one input. Ideally it should be the angle γ in the unitarity triangle determined in tree-level decays and therefore independently of $S(v)$. For this reason we present our results as functions of γ . However, as γ is presently not well known from tree-level decays, we will use the range for the ratio

$$\xi = \frac{F_{B_s}\sqrt{\hat{B}_{B_s}}}{F_{B_d}\sqrt{\hat{B}_{B_d}}} \quad (5)$$

from lattice calculations to find out which range for γ is consistent with experimental value of the ratio $\Delta M_s/\Delta M_d$ in the full class of CMFV models independently of $S(v)$.

In principle, also $|V_{cb}|$ could be used as input, but the very strong dependence of ε_K on $|V_{cb}|$ as $|V_{cb}|^4$ invites us in the presence of an accurate value of \hat{B}_K to determine $|V_{cb}|$ from ε_K ¹. As already stated above we determine here $|V_{cb}|$ to fit FCNC data and this makes sense in this concrete class of models. Comparison with tree-level results for $|V_{cb}|$ will offer still another test of CMFV.

Our paper is organized as follows. In Section 2 we recall the formulae used in our analysis. In Section 3 we calculate

$$|V_{cb}|, \quad F_{B_s}\sqrt{\hat{B}_{B_s}}, \quad F_{B_d}\sqrt{\hat{B}_{B_d}}, \quad |V_{ub}|, \quad |V_{td}|, \quad |V_{ts}|, \quad \mathcal{B}(B^+ \rightarrow \tau^+ \nu_\tau) \quad (6)$$

¹The idea of determining $|V_{cb}|$ from ε_K is not new. It was suggested in [32] with the goal to predict an accurate value of $\mathcal{B}(K^+ \rightarrow \pi^+ \nu \bar{\nu})$ within the SM that similarly to ε_K suffers from $|V_{cb}|^4$ dependence. But at that time the precision on \hat{B}_K was insufficient so that this strategy could not be used efficiently.

in CMFV models as functions of $S(v)$ and γ . Among these models a prominent role is played by the SM. These results will be compared in the future with more precise values of these quantities but already now one can see that CMFV models will have hard time to give a satisfactory description of them unless very significant differences from the present values of $|V_{cb}|$, $F_{B_s}\sqrt{\hat{B}_{B_s}}$ and $F_{B_d}\sqrt{\hat{B}_{B_d}}$ will be found. In Section 4 we analyze the uncertainty in the determination of $|V_{cb}|$ induced by the large uncertainty in the QCD factor η_{cc} in the charm contribution to ε_K . We demonstrate how this uncertainty can be reduced by a factor of three by using the experimental value of ΔM_K and the large N estimate of long distance contributions to the latter. In Section 5 we address simplest models outside the CMFV framework, in particular the MFV models at large, where new operators and flavour blind phases could be present. We also comment on models with $U(2)^3$ flavour symmetry. In Section 6 we summarize briefly our results.

2 Compendium of Basic Formulae

2.1 $\Delta F = 2$ Observables

Here we collect the formulae we used in our calculations. For the mass differences in the $B_{s,d}^0 - \bar{B}_{s,d}^0$ systems we have

$$\Delta M_s = 19.1/\text{ps} \cdot \left[\frac{\sqrt{\hat{B}_{B_s}} F_{B_s}}{279 \text{ MeV}} \right]^2 \left[\frac{S(v)}{2.31} \right] \left[\frac{|V_{ts}|}{0.040} \right]^2 \left[\frac{\eta_B}{0.55} \right], \quad (7)$$

$$\Delta M_d = 0.55/\text{ps} \cdot \left[\frac{\sqrt{\hat{B}_{B_d}} F_{B_d}}{226 \text{ MeV}} \right]^2 \left[\frac{S(v)}{2.31} \right] \left[\frac{|V_{td}|}{8.5 \cdot 10^{-3}} \right]^2 \left[\frac{\eta_B}{0.55} \right]. \quad (8)$$

The value 2.31 in the normalization of $S(v)$ is its present SM value for $\bar{m}_t(m_t) = 163 \text{ GeV}$:

$$S_0(x_t) = \frac{4x_t - 11x_t^2 + x_t^3}{4(1-x_t)^2} - \frac{3x_t^2 \log x_t}{2(1-x_t)^3} = 2.31 \left[\frac{\bar{m}_t(m_t)}{163 \text{ GeV}} \right]^{1.52}. \quad (9)$$

Concerning $|V_{td}|$ and $|V_{ts}|$, we have first

$$|V_{td}| = |V_{us}| |V_{cb}| R_t \quad (10)$$

with R_t being one of the length of the unitarity triangle which generally in CMFV can be determined independently of $S(v)$ [3]:

$$R_t = \eta_R \frac{\xi}{|V_{us}|} \sqrt{\frac{\Delta M_d}{\Delta M_s}} \sqrt{\frac{m_{B_s}}{m_{B_d}}}, \quad \eta_R = 1 - |V_{us}| \xi \sqrt{\frac{\Delta M_d}{\Delta M_s}} \sqrt{\frac{m_{B_s}}{m_{B_d}}} \cos \beta + \frac{\lambda^2}{2} + \mathcal{O}(\lambda^4). \quad (11)$$

Here ξ is defined in (5) and β is determined also universally through (2). We also have

$$|V_{ts}| = \eta_R |V_{cb}| \quad (12)$$

with $|V_{cb}|$ determined from ε_K as discussed below.

Now the departure of η_R from unity is very small and can be calculated by using present lattice input for ξ and the central value of β . This gives

$$R_t = 0.743 \, \xi, \quad \eta_R = 0.9812 . \quad (13)$$

For the numerics in Section 3 we however use the relation (11) without the lattice input, except for Eq. (29) below where we use (13).

The next steps depend on whether ξ or γ is used as an input. If ξ is used, (13) allows to determine R_t and using the relations

$$R_b = \left(1 - \frac{\lambda^2}{2}\right) \frac{1}{\lambda} \left| \frac{V_{ub}}{V_{cb}} \right| = \sqrt{1 + R_t^2 - 2R_t \cos \beta}, \quad \cot \gamma = \frac{1 - R_t \cos \beta}{R_t \sin \beta} . \quad (14)$$

allows to determine $|V_{ub}|$ and γ .

On the other hand if γ from tree level decays is used as an input, one could determine R_t and R_b without using the lattice value of ξ [33]:

$$R_t = \frac{\sin \gamma}{\sin(\beta + \gamma)}, \quad R_b = \frac{\sin \beta}{\sin(\beta + \gamma)} . \quad (15)$$

In turn ξ could be determined by using (11) and the comparison with its lattice value would be another test of CMFV.

Finally, the CP-violating parameter ε_K is given by

$$\varepsilon_K = \frac{\kappa_\varepsilon e^{i\varphi_\varepsilon}}{\sqrt{2}(\Delta M_K)_{\text{exp}}} [\Im(M_{12}^K)] , \quad (16)$$

where $\varphi_\varepsilon = (43.51 \pm 0.05)^\circ$ and $\kappa_\varepsilon = 0.94 \pm 0.02$ [6, 34] takes into account that $\varphi_\varepsilon \neq \frac{\pi}{4}$ and includes long distance effects in $\Im(\Gamma_{12})$ and $\Im(M_{12}^K)$. Moreover ($\lambda_i = V_{is}^* V_{id}$)

$$(M_{12}^K)^* = \frac{G_F^2}{12\pi^2} F_K^2 \hat{B}_K m_K M_W^2 [\lambda_c^2 \eta_{cc} S_0(x_c) + \lambda_t^2 \eta_{tt} S(v) + 2\lambda_c \lambda_t \eta_{ct} S_0(x_c, x_t)] , \quad (17)$$

where the QCD factors η_{ij} are given in Table 1 and $S_0(x_c, x_t)$ can be found in [35]. In writing (17) we make a very plausible assumption that in models with CMFV, NP enters only through $S(v)$. In any case the contributions involving charm quark are subleading.

We can then expose the main parametric dependence of ε_K within the CMFV models as follows [6]:

$$|\varepsilon_K| = \kappa_\varepsilon C_\varepsilon \hat{B}_K |V_{cb}|^2 \lambda^2 \bar{\eta} (|V_{cb}|^2 (1 - \bar{\rho}) \eta_{tt} S(v) + \eta_{ct} S_0(x_c, x_t) - \eta_{cc} x_c) , \quad (18)$$

where $\bar{\eta}$ and $\bar{\varrho}$ are the known variables related to the unitarity triangle and

$$C_\varepsilon = \frac{G_F^2 F_K^2 m_K M_W^2}{6\sqrt{2}\pi^2 (\Delta M_K)_{\text{exp}}}. \quad (19)$$

As in ε_K the function $S(v)$ is proportional to $|V_{cb}|^4$ and not $|V_{cb}|^2$ as in $\Delta M_{s,d}$ it is ε_K which plays the crucial role in fixing the favoured value of $|V_{cb}|$. The prime roles of $\Delta M_{s,d}$ is to determine R_t through (11) and then $F_{B_s}\sqrt{\hat{B}_{B_s}}$ and $F_{B_d}\sqrt{\hat{B}_{B_d}}$ through (7) and (8), respectively.

Finally, eliminating $S(v)$ from all these expressions in terms of other variables we find the basic formula expressing the correlation between various quantities discussed in our paper

$$S_{\psi K_S} = \sin 2\beta = \frac{1}{b\Delta M_d} \left[\frac{|\varepsilon_K|}{|V_{cb}|^2 \hat{B}_K} - a \right], \quad (20)$$

where

$$a = r_\varepsilon R_t \sin \beta [\eta_{ct} S_0(x_t, x_c) - \eta_{cc} x_c], \quad b = \frac{\eta_{tt}}{\eta_B} \frac{r_\varepsilon}{2r_d |V_{us}|^2} \frac{1}{F_{B_d}^2 \hat{B}_{B_d}}, \quad (21)$$

with

$$r_\varepsilon = \kappa_\varepsilon |V_{us}|^2 C_\varepsilon, \quad r_d = \frac{G_F^2}{6\pi^2} M_W^2 m_{B_d} \quad (22)$$

and R_t given in (11).

In the derivation of (20) the following relations are useful

$$\sin 2\beta = 2 \frac{\bar{\eta}(1 - \bar{\varrho})}{R_t^2}, \quad \bar{\eta} = R_t \sin \beta. \quad (23)$$

2.2 $B^+ \rightarrow \tau^+ \nu$ in CMFV

It will also be interesting to consider the tree-level decay $B^+ \rightarrow \tau^+ \nu_\tau$. In the SM $B^+ \rightarrow \tau^+ \nu_\tau$ is mediated by the W^\pm exchange with the resulting branching ratio given by

$$\mathcal{B}(B^+ \rightarrow \tau^+ \nu_\tau)_{\text{SM}} = \frac{G_F^2 m_{B^+} m_\tau^2}{8\pi} \left(1 - \frac{m_\tau^2}{m_{B^+}^2} \right)^2 F_{B^+}^2 |V_{ub}|^2 \tau_{B^+} = 6.05 |V_{ub}|^2 \left(\frac{F_{B^+}}{185 \text{ MeV}} \right)^2. \quad (24)$$

Evidently this result is subject to significant parametric uncertainties induced in (24) by F_{B^+} and $|V_{ub}|$. However, recently the error on F_{B^+} from lattice QCD decreased significantly [36] so that the dominant uncertainty comes from $|V_{ub}|$.

To our knowledge $B^+ \rightarrow \tau^+ \nu_\tau$ decay has never been considered in CMFV. Here we would like to point out that in this class of models the branching ratio for this decay is

enhanced (suppressed) for the same (opposite) sign of the lepton coupling of the new charged gauge boson relative to the SM one. Indeed, the only possibility to modify the SM result up to loop corrections in CMFV is through a tree-level exchange of a new charged gauge boson, whose flavour interactions with quarks are governed by the CKM matrix. In particular the operator structure is the same.

Denoting this gauge boson by W' and the corresponding gauge coupling by \tilde{g}_2 one has

$$\frac{\mathcal{B}(B^+ \rightarrow \tau^+ \nu)}{\mathcal{B}(B^+ \rightarrow \tau^+ \nu)^{\text{SM}}} = \left(1 + r \frac{\tilde{g}_2^2}{g_2^2} \frac{M_W^2}{M_{W'}^2}\right)^2, \quad (25)$$

where we introduced a factor r allowing a modification in the lepton couplings relatively to the SM ones, in particular of its sign. Which sign is required will be known once the data and SM prediction improve.

If W' with these properties is absent, the branching ratio in this framework is not modified with respect to the SM up to loop corrections that could involve new particles but are expected to be small. A tree-level H^\pm exchange generates new operators and is outside this framework. In order to simplify the analysis, in what follows we will neglect direct NP contributions to this decay and we will use the SM formula (24). In this manner NP will enter this decay indirectly through the value of $|V_{ub}|$ determined in our $\Delta F = 2$ analysis.

3 Numerical Analysis

Our analysis uses the inputs of Table 1 where we also collect the present values of the quantities in (3) that we will determine. In this context let us emphasize that while the results for weak decay constants from lattice are very new, the values of $F_{B_s} \sqrt{\hat{B}_{B_s}}$, $F_{B_d} \sqrt{\hat{B}_{B_d}}$, \hat{B}_{B_s} and \hat{B}_{B_d} given in this Table are from 2011. But soon these results should be updated. Still it is tempting to combine the new results for weak decay constants with the values of the \hat{B}_i parameters in Table 1 to find

$$F_{B_s} \sqrt{\hat{B}_{B_s}} = 259(7) \text{ MeV}, \quad F_{B_d} \sqrt{\hat{B}_{B_d}} = 211(10) \text{ MeV}, \quad \xi = 1.227. \quad (26)$$

We observe that ξ is basically unchanged but the values of $F_{B_s} \sqrt{\hat{B}_{B_s}}$ and $F_{B_d} \sqrt{\hat{B}_{B_d}}$ are decreased. Consequently as investigated in [10] also ΔM_s and ΔM_d decrease so that the $\varepsilon_K - \Delta M_{s,d}$ tension in CMFV identified in [10, 11] would be softened. But this requires the confirmation of the values in (26) by future lattice calculations.

Before entering our analysis we want to find the range for γ by using the range for ξ in Table 1 together with formulae (11) and (14). We find independently of $S(v)^2$

$$\gamma = (66.6 \pm 3.7)^\circ \quad (\text{CMFV}) \quad (27)$$

²We included the uncertainty from $S_{\psi K_S}$ as well.

| | | | |
|---|----------|--|----------|
| $G_F = 1.16637(1) \times 10^{-5} \text{ GeV}^{-2}$ | [37] | $m_{B_d} = m_{B^+} = 5279.2(2) \text{ MeV}$ | [38] |
| $M_W = 80.385(15) \text{ GeV}$ | [37] | $m_{B_s} = 5366.8(2) \text{ MeV}$ | [38] |
| $\sin^2 \theta_W = 0.23116(13)$ | [37] | $F_{B_d} = (188 \pm 4) \text{ MeV}$ | [36] |
| $\alpha(M_Z) = 1/127.9$ | [37] | $F_{B_s} = (225 \pm 3) \text{ MeV}$ | [36] |
| $\alpha_s(M_Z) = 0.1184(7)$ | [37] | $F_{B^+} = (185 \pm 3) \text{ MeV}$ | [36] |
| $m_u(2 \text{ GeV}) = (2.1 \pm 0.1) \text{ MeV}$ | [20] | $\hat{B}_{B_d} = 1.26(11), \hat{B}_{B_s} = 1.33(6)$ | [20] |
| $m_d(2 \text{ GeV}) = (4.73 \pm 0.12) \text{ MeV}$ | [20] | $\hat{B}_{B_s}/\hat{B}_{B_d} = 1.05(7)$ | [20] |
| $m_s(2 \text{ GeV}) = (93.4 \pm 1.1) \text{ MeV}$ | [20] | $F_{B_d} \sqrt{\hat{B}_{B_d}} = 226(13) \text{ MeV}$ | [20] |
| $m_c(m_c) = (1.279 \pm 0.013) \text{ GeV}$ | [39] | $F_{B_s} \sqrt{\hat{B}_{B_s}} = 279(13) \text{ MeV}$ | [20] |
| $m_b(m_b) = 4.19_{-0.06}^{+0.18} \text{ GeV}$ | [37] | $\xi = 1.237(32)$ | [20] |
| $m_t(m_t) = 163(1) \text{ GeV}$ | [20, 40] | $\eta_B = 0.55(1)$ | [41, 42] |
| $M_t = 173.2 \pm 0.9 \text{ GeV}$ | [43] | $\Delta M_d = 0.507(4) \text{ ps}^{-1}$ | [44] |
| $m_K = 497.614(24) \text{ MeV}$ | [37] | $\Delta M_s = 17.72(4) \text{ ps}^{-1}$ | [44] |
| $F_K = 156.1(11) \text{ MeV}$ | [20] | $S_{\psi K_S} = 0.679(20)$ | [37] |
| $\hat{B}_K = 0.767(10)$ | [20] | $S_{\psi\phi} = -0.01 \pm 0.08$ | [45] |
| $\kappa_\epsilon = 0.94(2)$ | [6, 34] | $\Delta\Gamma_s = 0.116 \pm 0.019$ | [46] |
| $\eta_{cc} = 1.87(76)$ | [47] | $\tau_{B_s} = 1.503(10) \text{ ps}$ | [44] |
| $\eta_{tt} = 0.5765(65)$ | [41] | $\tau_{B_d} = 1.519(7) \text{ ps}$ | [44] |
| $\eta_{ct} = 0.496(47)$ | [48] | $\tau_{B^\pm} = (1641 \pm 8) \times 10^{-3} \text{ ps}$ | [44] |
| $\Delta M_K = 0.5292(9) \times 10^{-2} \text{ ps}^{-1}$ | [37] | $ V_{us} = 0.2252(9)$ | [44] |
| $ \varepsilon_K = 2.228(11) \times 10^{-3}$ | [37] | $ V_{cb} = (40.9 \pm 1.1) \times 10^{-3}$ | [38] |
| $\mathcal{B}(B \rightarrow X_s \gamma) = (3.55 \pm 0.24 \pm 0.09) \times 10^{-4}$ | [37] | $ V_{ub}^{\text{incl.}} = (4.41 \pm 0.31) \times 10^{-3}$ | [38] |
| $\mathcal{B}(B^+ \rightarrow \tau^+ \nu) = (0.99 \pm 0.25) \times 10^{-4}$ | [49] | $ V_{ub}^{\text{excl.}} = (3.23 \pm 0.31) \times 10^{-3}$ | [38] |

Table 1: *Values of the experimental and theoretical quantities used as input parameters.*

which having much smaller error agrees very well with γ from tree-level decays obtained by LHCb

$$\gamma = (67.2 \pm 12)^\circ, \quad (\text{LHCb}) . \quad (28)$$

Similar comment applies to the extraction of γ from U-spin analysis of $B_s \rightarrow K^+ K^-$ and $B_d \rightarrow \pi^+ \pi^-$ decays ($\gamma = (68.2 \pm 7.1)^\circ$) [50].

In our paper guided by the range in (27) we will proceed in the following steps³:

Step 1: For a given γ and β from $S_{\psi K_S}$ we will calculate R_b and R_t by means of (15) and subsequently ξ by using (11).

Step 2: Having ξ allows with the help of ϵ_K to determine $|V_{cb}|$ as a function of $S(v)$.

³The numerical values in the expressions in this section correspond to the central values of the remaining input parameters.

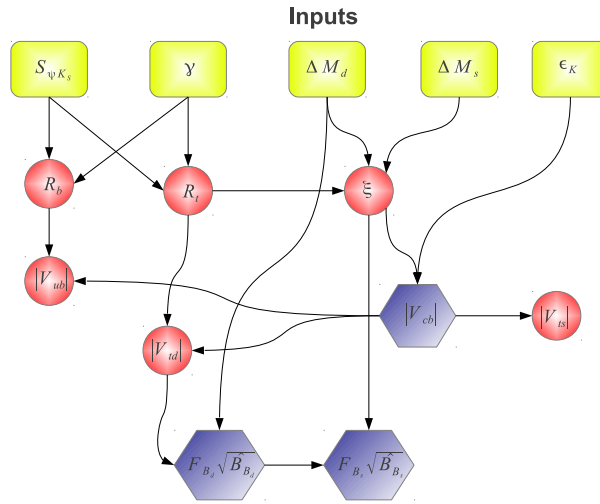


Figure 1: *The overview of the determination of various quantities discussed in the text with results given in Table 2.*

Explicitly for central values of parameters we find (using (13))

$$|V_{cb}| = \frac{v(\eta_{cc}, \eta_{ct})}{\sqrt{\xi S(v)}} \sqrt{\sqrt{1 + h(\eta_{cc}, \eta_{ct}) S(v)} - 1}, \quad v(\eta_{cc}, \eta_{ct}) = 0.0282, \quad h(\eta_{cc}, \eta_{ct}) = 24.83. \quad (29)$$

The second solution of the quadratic equation for $|V_{cb}|^2$ is excluded as it leads to a negative $|V_{cb}|^2$. The numerical values of $h(\eta_{cc}, \eta_{ct})$ and $v(\eta_{cc}, \eta_{ct})$ correspond to the central values of η_{cc} and η_{ct} in Table 1. We will discuss the uncertainty due to these parameters in the next section.

With all this information at hand we can determine $|V_{ub}|$, $|V_{ts}|$ and $|V_{td}|$ as functions of $S(v)$.

Step 3: Finally having $|V_{cb}|$ we can determine $\sqrt{\hat{B}_{B_d}} F_{B_d}$ from (8) and knowing already ξ from Step 1 also $\sqrt{\hat{B}_{B_s}} F_{B_s}$.

As the route to determine all these quantities could appear not transparent we show it in a chart in Fig. 1.

In Fig. 2 we show the dependence of ξ on γ varying $S_{\psi K_S}$ in its one σ range. We note that the uncertainty due to $S_{\psi K_S}$ is very small. This triple correlation is universal for all CMFV models including the SM and is central for tests of CMFV framework. Measuring γ from tree-level decays precisely together with precise values of $S_{\psi K_S}$ and ξ will be an important test for this class of models as this correlation is independent of $S(v)$. The range for γ in (27) has been extracted from this plot by varying ξ and $S_{\psi K_S}$ independently in their present one σ ranges.

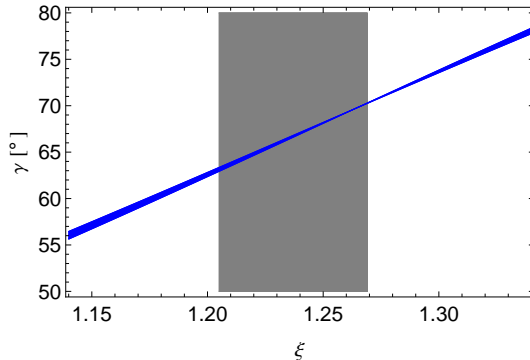


Figure 2: γ versus ξ for $S_{\psi K_S} \in [0.659, 0.699]$.

It should be emphasized that this first test is independent of $|V_{ub}|$ and $|V_{cb}|$ and can become a precision test of CMFV models. But in order to find out which CMFV model, if any, is chosen by nature we have to consider the quantities which depend on $S(v)$. This brings us to Steps 2 and 3.

The $S(v)$ and γ dependence of all quantities of interest is shown in Table 2. We show there also the SM case corresponding to $S(v) = S_0(x_t) = 2.31$. These results are also shown in Fig. 3, where we plot various quantities as functions of $S(v)$ for different values of γ . The thickness of the lines shows the uncertainty in $S_{\psi K_S}$. Evidently these plots are correlated with each other:

- Once one of the variables is determined, also $S(v)$ is determined and consequently the remaining quantities are predicted.
- In a given model in which $S(v)$ is known, all quantities considered are predicted.

Equivalently to Fig. 3 one can find using (20) explicit universal correlations between various quantities in Table 2. We show few examples below. In all plots we also show the present best values of all quantities obtained directly from lattice or tree-level decays.

In order to understand the results in Table 2 let us recall the problems of CMFV for the present input for $|V_{cb}|$, $F_{B_s}\sqrt{\hat{B}_{B_s}}$ and $F_{B_d}\sqrt{\hat{B}_{B_d}}$ in Table 1 [10, 11]. With the value of β extracted from $S_{\psi K_S}$ and γ from $\Delta M_s/\Delta M_d$, ε_K is in the SM significantly smaller than its experimental value, while $\Delta M_{s,d}$ are significantly larger than corresponding experimental values. Therefore increasing $S(v)$, while bringing ε_K closer to the data, shifts $\Delta M_{s,d}$ further from their experimental values. Using for example $|V_{ub}| = 0.0034$ and $\gamma = 68^\circ$ where the SM prediction and the central experimental value for $S_{\psi K_S}$ coincide, the SM prediction for $|\varepsilon_K|^{\text{SM}} = 0.00186$ is below the data. Turning now to CMFV, the value of $S(v)$ at which the central experimental value of $|\varepsilon_K|$ is reproduced turns out to be $S(v) = 2.9$ [11] to be compared with $S_{\text{SM}} = 2.31$. At this value of $S(v)$ with present input the central values of $\Delta M_{s,d}$ read

$$\Delta M_d = 0.69(6) \text{ ps}^{-1}, \quad \Delta M_s = 23.9(2.1) \text{ ps}^{-1}. \quad (30)$$

| $S(v)$ | γ | $ V_{cb} $ | $ V_{ub} $ | $ V_{td} $ | $ V_{ts} $ | $F_{B_s}\sqrt{\hat{B}_{B_s}}$ | $F_{B_d}\sqrt{\hat{B}_{B_d}}$ | ξ | $\mathcal{B}(B^+ \rightarrow \tau^+\nu)$ |
|--------|----------|------------|------------|------------|------------|-------------------------------|-------------------------------|-------|--|
| 2.31 | 63° | 43.6 | 3.69 | 8.79 | 42.8 | 252.7 | 210.0 | 1.204 | 0.822 |
| 2.5 | 63° | 42.8 | 3.63 | 8.64 | 42.1 | 247.1 | 205.3 | 1.204 | 0.794 |
| 2.7 | 63° | 42.1 | 3.56 | 8.49 | 41.4 | 241.8 | 200.9 | 1.204 | 0.768 |
| 2.31 | 67° | 42.9 | 3.62 | 8.90 | 42.1 | 256.8 | 207.2 | 1.240 | 0.791 |
| 2.5 | 67° | 42.2 | 3.56 | 8.75 | 41.4 | 251.1 | 202.6 | 1.240 | 0.765 |
| 2.7 | 67° | 41.5 | 3.50 | 8.61 | 40.7 | 245.7 | 198.3 | 1.240 | 0.739 |
| 2.31 | 71° | 42.3 | 3.57 | 9.02 | 41.5 | 260.8 | 204.5 | 1.276 | 0.770 |
| 2.5 | 71° | 41.6 | 3.51 | 8.87 | 40.8 | 255.1 | 200.0 | 1.276 | 0.744 |
| 2.7 | 71° | 40.9 | 3.45 | 8.72 | 40.1 | 249.6 | 195.7 | 1.276 | 0.719 |

Table 2: *CMFV predictions for various quantities as functions of $S(v)$ and γ . The four elements of the CKM matrix are in units of 10^{-3} , $F_{B_s}\sqrt{\hat{B}_{B_s}}$ and $F_{B_d}\sqrt{\hat{B}_{B_d}}$ in units of MeV and $\mathcal{B}(B^+ \rightarrow \tau^+\nu)$ in units of 10^{-4} .*

They both differ from experimental values by 3σ . Using another value of $|V_{ub}|$ which worsen the agreement of the SM with the experimental value for $S_{\psi K_S}$ leads to a different value of $S(v)$ to reproduce $|\varepsilon_K|^{\text{exp}} = 0.002228$ and thus also (30) changes.

These problems of CMFV can also be seen when the present central values of $|V_{cb}|$ and of non-perturbative parameters are inserted together with the data on $\Delta M_{s,d}$, ε_K , $|V_{cb}|$ and $|V_{us}|$ into (20). We find then

$$S_{\psi K_S} = \sin 2\beta = 0.86 \Rightarrow \beta = 29.8^\circ, \quad R_t = 0.92 \quad (31)$$

and thus

$$R_b = 0.50, \quad |V_{ub}| = 0.0047, \quad \gamma = 66.4^\circ. \quad (32)$$

Evidently, the fact that $S_{\psi K_S}$ is much larger than the data requires the presence of new CP-violating phases. This exercise is equivalent to the one performed in [5], where ε_K has been set to its experimental value but $\sin 2\beta$ was predicted. On the other hand setting $S_{\psi K_S}$ to its experimental value as done in [6] one finds that $|\varepsilon_K|$ is significantly below the data.

Thus the only hope for CMFV is that the input on $|V_{cb}|$, $F_{B_s}\sqrt{\hat{B}_{B_s}}$ and $F_{B_d}\sqrt{\hat{B}_{B_d}}$ changes with time. In particular as seen in Table 2:

- The values of $F_{B_s}\sqrt{\hat{B}_{B_s}}$ and $F_{B_d}\sqrt{\hat{B}_{B_d}}$ have to decrease significantly, at least as far as given in (26). But this assumes the lowest value of $S(v)$.

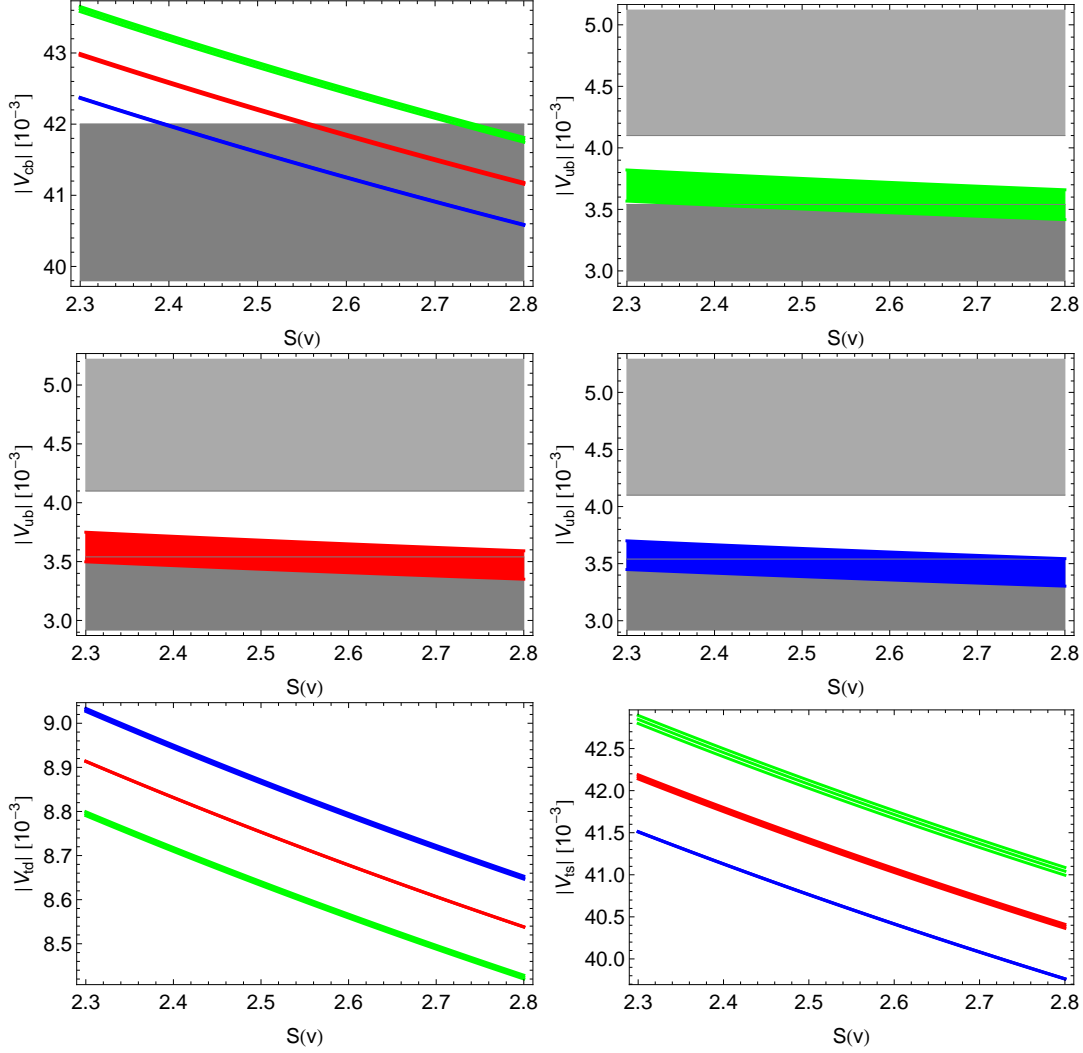


Figure 3: *CKM matrix elements versus $S(v)$ for $\gamma = 63^\circ/67^\circ/71^\circ$ (green, red, blue). The thickness of the lines corresponds to the 1σ range of $S_{\psi K_S} \in [0.659, 0.699]$.*

- At this value of $S(v)$ in order to obtain agreement of ε_K with the data $|V_{cb}|$ should be larger by roughly 2σ from its present tree-level value.
- Increasing $S(v)$ allows to lower the required value of $|V_{cb}|$ but simultaneously decreases further $F_{B_s}\sqrt{\hat{B}_{B_s}}$ and $F_{B_d}\sqrt{\hat{B}_{B_d}}$ making their values significantly lower than their present values without changing their ratio (see Fig. 4). This finding shows that the freedom in choosing $S(v)$ does not necessarily help in solving CMFV problems.
- With increasing γ the value of $|V_{cb}|$ required by ε_K can further be decreased. For a fixed $S(v)$ this increases $F_{B_s}\sqrt{\hat{B}_{B_s}}$ but decreases $F_{B_d}\sqrt{\hat{B}_{B_d}}$ as can be read off

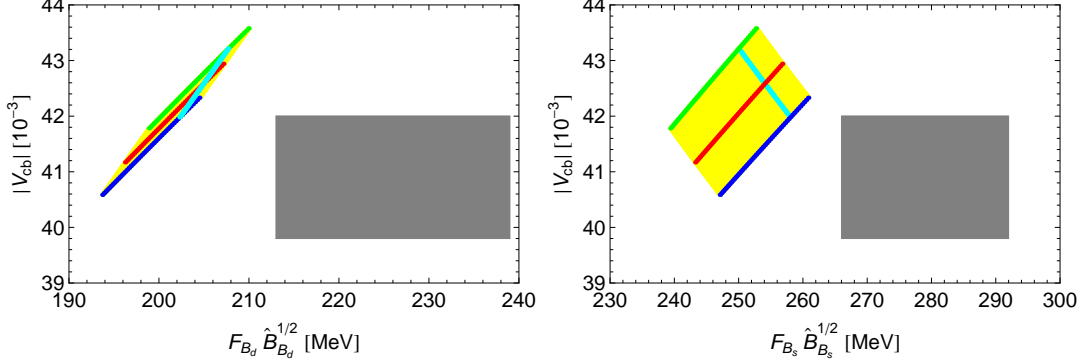


Figure 4: $|V_{cb}|$ versus $F_{B_d}\sqrt{\hat{B}_{B_d}}$ and $F_{B_s}\sqrt{\hat{B}_{B_s}}$ for $S(v) \in [2.3, 2.8]$ and $\gamma \in [63^\circ, 71^\circ]$ (yellow), $\gamma = 63^\circ/67^\circ/71^\circ$ (green, red, blue). Cyan: fixed $S(v) = 2.4$ and $\gamma \in [63^\circ, 71^\circ]$. Gray range: 1σ range of $F_{B_d}\sqrt{\hat{B}_{B_d}} = 226(13)$ MeV, $F_{B_s}\sqrt{\hat{B}_{B_s}} = 279(13)$ MeV and $|V_{cb}| = (40.9 \pm 1.1) \times 10^{-3}$ (see Table 1).

from Fig. 4.

- For the full range of $S(v)$ and γ considered in Table 2 the values of $|V_{ub}|$ and $|V_{td}|$ remain in the following ranges:

$$|V_{ub}| = (3.57 \pm 0.16) \times 10^{-3}, \quad |V_{td}| = (8.75 \pm 0.26) \times 10^{-3} \quad (33)$$

where in the case of $|V_{ub}|$ we included also the error from β , which is irrelevant in the case of $|V_{td}|$. Otherwise the error in $|V_{ub}|$ would amount to ± 0.12 . The value of $|V_{ts}|$ follows the one of $|V_{cb}|$ but is by 1.9% smaller than the latter. Also for $\mathcal{B}(B^+ \rightarrow \tau^+ \nu)$ a narrow range is predicted:

$$\mathcal{B}(B^+ \rightarrow \tau^+ \nu) = (0.77 \pm 0.07) \times 10^{-4}, \quad (34)$$

where the present uncertainty in F_{B^+} has been taken into account.

In Fig. 4 on the left hand side we show the correlation between $F_{B_d}\sqrt{\hat{B}_{B_d}}$ and $|V_{cb}|$ for different value of γ . Analogous correlation between $F_{B_s}\sqrt{\hat{B}_{B_s}}$ and $|V_{cb}|$ is shown on the right hand side. Possibly these two plots showing the allowed ranges for the three parameters in question in the CMFV framework are the most important result of our paper. Similarly we show in Fig. 5 the same correlation but with $|V_{ub}|$.

4 The Uncertainty due to η_{cc} and η_{ct}

It is known that significant uncertainty in the SM prediction for ε_K comes from the value of the QCD correction η_{cc} and to a lesser extent from η_{ct} that even at the NNLO

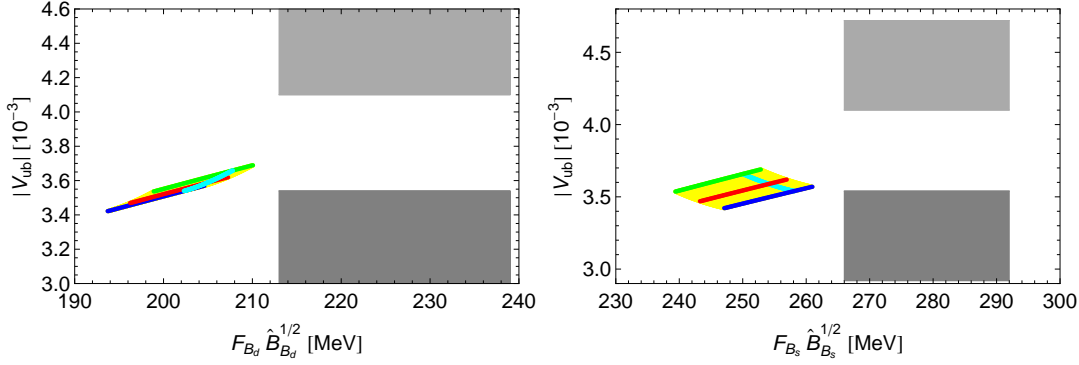


Figure 5: $|V_{ub}|$ versus $F_{B_d}\sqrt{\hat{B}_{B_d}}$ and $F_{B_s}\sqrt{\hat{B}_{B_s}}$ for $S(v) \in [2.3, 2.8]$ and $\gamma \in [63^\circ, 71^\circ]$ (yellow), $\gamma = 63^\circ/67^\circ/71^\circ$ (green, red, blue). Cyan: fixed $S(v) = 2.4$ and $\gamma \in [63^\circ, 71^\circ]$. Gray range: 1σ range of $F_{B_d}\sqrt{\hat{B}_{B_d}} = 226(13)$ MeV, $F_{B_s}\sqrt{\hat{B}_{B_s}} = 279(13)$ MeV and $|V_{ub}^{excl}| = (3.21 \pm 0.31) \times 10^{-3}$ (light gray), $|V_{ub}^{incl}| = (4.41 \pm 0.31) \times 10^{-3}$ (dark gray) (see Table 1).

| $h(\eta_{cc}, \eta_{ct})$ | | η_{cc} | | | $v(\eta_{cc}, \eta_{ct})$ | | η_{cc} | | |
|---------------------------|-------|-------------|-------|-------|---------------------------|-------|-------------|--------|--------|
| | | 1.10 | 1.87 | 2.64 | | | 1.10 | 1.87 | 2.64 |
| η_{ct} | 0.451 | 18.83 | 34.93 | 85.82 | η_{ct} | 0.451 | 0.0303 | 0.0259 | 0.0207 |
| | 0.496 | 15.57 | 24.83 | 51.42 | | 0.496 | 0.0323 | 0.0282 | 0.0235 |
| | 0.541 | 11.61 | 18.55 | 34.21 | | 0.541 | 0.0341 | 0.0304 | 0.0260 |

Table 3: Coefficient $h(\eta_{cc}, \eta_{ct})$ and $v(\eta_{cc}, \eta_{ct})$ in Eq. (29) for different values of $\eta_{cc,ct}$.

level are known only with the accuracy of $\pm 41\%$ and $\pm 9\%$, respectively [47, 48]. In our analysis this uncertainty enters the coefficient $h(\eta_{cc}, \eta_{ct})$ of $S(v)$ and $v(\eta_{cc}, \eta_{ct})$ in (29). In what follows we would like to investigate the impact of these uncertainties on the determination of $|V_{cb}|$ from ε_K and propose a method how the uncertainty in η_{cc} could be reduced with the help of the experimental value of ΔM_K accompanied in particular by future lattice calculations of long distance effects in ΔM_K .

In Table 3 we show the values of $h(\eta_{cc}, \eta_{ct})$ corresponding to the range of these QCD corrections calculated in [47, 48]. If we fix $\gamma = 67^\circ$ and $S(v) = S_0(x_t) = 2.31$ and vary $\eta_{cc} \in [1.10, 2.64]$ and $\eta_{ct} \in [0.451, 0.541]$ simultaneously then $|V_{cb}|$ lies within the range $[41.7, 44.4] \cdot 10^{-3}$ (see also Fig. 6). Scanning only $\eta_{cc}(\eta_{ct})$ and fixing $\eta_{ct}(\eta_{cc})$ to its central value we find $|V_{cb}| \in [42.1, 43.9] \cdot 10^{-3}$ ($|V_{cb}| \in [42.6, 43.4] \cdot 10^{-3}$). Translated in the uncertainty in the determination of $|V_{cb}|$ we find an uncertainty of $\pm 2.0\%$ and $\pm 0.9\%$ due to η_{cc} and η_{ct} , respectively. The uncertainty due to η_{tt} is fully negligible. It is expected that an improved matching of short distance calculations of η_{cc} and η_{ct} to the lattice calculations of \hat{B}_K can significantly reduce the present total theoretical error on ε_K and thus allow a more accurate extraction of $|V_{cb}|$.

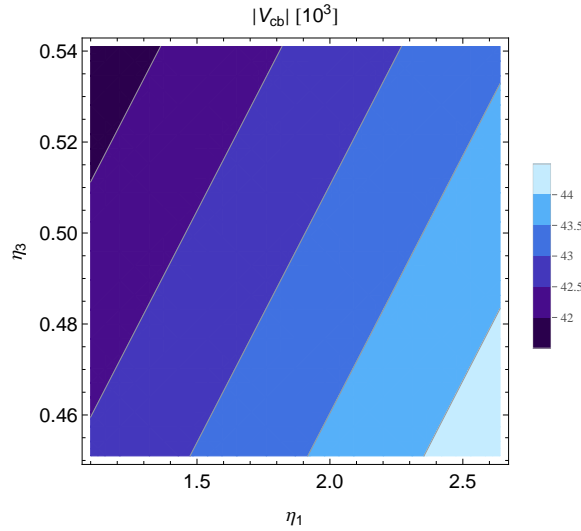


Figure 6: $|V_{cb}|$ as a function of η_{cc} and η_{ct} for fixed $\gamma = 67^\circ$ and $S(v) = S_0(x_t) = 2.31$.

As the large uncertainty in η_{cc} is disturbing we propose to extract this parameter from the experimental value of ΔM_K . Assuming that in CMFV models ΔM_K is fully dominated by the SM contributions we decompose it as follows:

$$\Delta M_K = (\Delta M_K)_{cc} + (\Delta M_K)_{ct} + (\Delta M_K)_{tt} + (\Delta M_K)_{LD}, \quad (35)$$

with the first three short distance contributions obtained from

$$(\Delta M_K)_{ij} = 2\Re(M_{12}^K)_{ij} \quad (36)$$

with M_{12}^K given in (17) and $i = c, t$. For the dominant contribution we have

$$(\Delta M_K)_{cc} = \left(\lambda - \frac{\lambda^3}{2}\right)^2 \frac{G_F^2}{6\pi^2} F_K^2 \hat{B}_K m_K \eta_{cc} m_c^2(m_c). \quad (37)$$

We find then setting $m_c(m_c)$ at its central value⁴

$$\eta_{cc} = 2.123 \left(\frac{0.75}{\hat{B}_K} \right) w, \quad (38)$$

where $(k = tt, ct, LD)$

$$w = 1 - r_{tt} - r_{ct} - r_{LD}, \quad r_k = \frac{(\Delta M_K)_k}{(\Delta M_K)_{\text{exp}}}. \quad (39)$$

⁴In principle the determination of $\eta_{cc}x_c$ is more useful as this product should be independent of the scale μ_c in m_c but in order to compare with the value of η_{cc} in Table 1 we prefer here to work with η_{cc} .

For r_{tt} and r_{ct} we find within the SM

$$r_{tt} = 0.0021, \quad r_{ct} = 0.0030 \quad (40)$$

confirming the result in [47] that both corrections are below 1% and totally negligible within the SM compared with other uncertainties. As our analysis shows in CMFV models r_{tt} could be increased by 30% due to the increase of $S(v)$ but this would still keep these corrections below 1%. Thus our proposal depends crucially on the estimate of r_{LD} . Yet, as we argue below the error from this contribution is significantly smaller than the error from the direct NNLO calculation in [47].

Basically the only results on r_{LD} in QCD that are available are from large N QCD calculations in which at low energies one uses a dual representation of QCD as a theory of weakly interacting mesons [51–53]. In the case of $K^0 - \bar{K}^0$ mixing and non-leptonic K -meson decays this approach, developed in [22, 23, 54–56], provided already a quarter of century ago results which are now basically confirmed by the more sophisticated lattice calculations. This is the case of the \hat{B}_K parameter calculated first in [22, 23] and also the case of $\Delta I = 1/2$ rule [56], where the dynamics behind this rule related predominantly to current-current operators has been identified and the enhancements of $\Delta I = 1/2$ transitions and suppression of $\Delta I = 3/2$ transitions have been computed reaching rough agreement with the data. Precisely this understanding is presently emerging from lattice calculations [57, 58].

Motivated by the success of this approach, its results for r_{LD} could also be approximately correct.. The leading in N contribution comes from one-loop contributions induced by two $\Delta S = 1$ transitions with virtual $\pi\pi$, πK and KK in the loop. One finds then r_{LD} to be *positive* and in the ballpark of 0.3 [59, 60]. The study of subleading corrections indicates that similarly to the case of \hat{B}_K these corrections are not large and tend to cancel partly each other [22, 34, 61, 62] with some tendency to have opposite sign to the leading term [62]. While precise calculation of r_{LD} in view of these cancellations is very difficult by analytic methods, based on these studies we expect that r_{LD} is likely to be positive and in the ballpark of 0.1 – 0.3. Taking this estimate at face value and using (38) we end up with

$$\eta_{cc} \approx 1.70 \pm 0.21. \quad (41)$$

This is consistent with $\eta_{cc} = 1.87$ used by us in the previous section. Moreover, the error is by a factor of 3-4 smaller than the error obtained by the direct NNLO calculation of η_{cc} in [47]. Interestingly the authors of the latter paper would find this result if they varied the scale μ_c in the range $1.3 \leq \mu_c \leq 1.8 \text{ GeV}$ and not in the range $1.0 - 2.0 \text{ GeV}$.

Needless to say, we are aware of the fact that these expectations and the estimate in (41) require more detailed investigations and in particular future confirmation from lattice simulations. Presently no reliable result on r_{LD} from lattice is available but an important progress towards its evaluation has been made in [63]. This first result seems to indicate that r_{LD} could be larger than expected by us. We are therefore looking forward to more precise evaluation of this important quantity from the lattice in order to see whether also in this case large N approach passed another test or not.

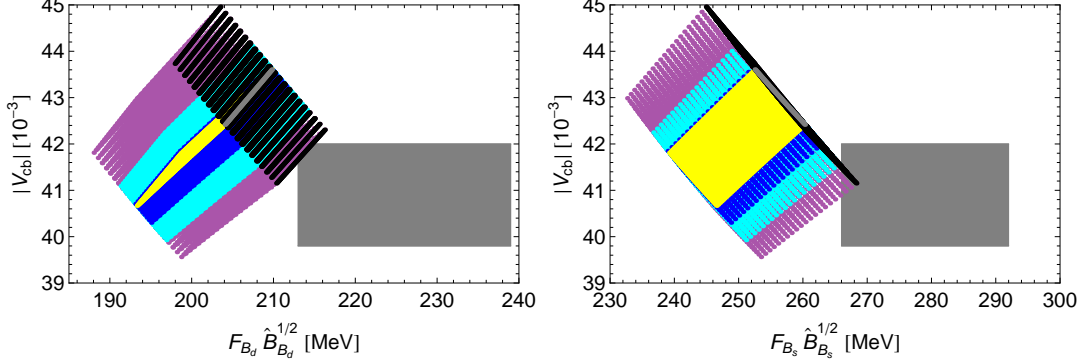


Figure 7: $|V_{cb}|$ versus $F_{B_d} \sqrt{\hat{B}_{B_d}}$ and $F_{B_s} \sqrt{\hat{B}_{B_s}}$ for $\gamma \in [63^\circ, 71^\circ]$. The yellow region is the same as in Fig. 4: $S(v) \in [2.31, 2.8]$, $\eta_{cc} = 1.87$, $\eta_{ct} = 0.496$. In the purple region we include the errors in $\eta_{cc,ct}$ as in Table 3: $S(v) \in [2.31, 2.8]$, $\eta_{cc} \in [1.10, 2.64]$, $\eta_{ct} \in [0.451, 0.541]$. In the cyan region we use instead the reduced error of η_{cc} as in Eq. (41): $S(v) \in [2.31, 2.8]$, $\eta_{cc} \in [1.49, 1.91]$, $\eta_{ct} \in [0.451, 0.541]$. In the blue region we fix η_{ct} to its central value: $S(v) \in [2.31, 2.8]$, $\eta_{cc} \in [1.49, 1.91]$, $\eta_{ct} = 0.496$. To test the SM we include the black region for fixed $S(v) = S_0(x_t) = 2.31$ and $\eta_{cc,ct}$ as in the purple region. The gray line within the black SM region corresponds to $\eta_{cc} = 1.87$ and $\eta_{ct} = 0.496$. The gray box is the same as in Fig. 4.

In Fig. 7 we show the anatomy of various uncertainties with different ranges described in the figure caption. We observe that the reduced error on η_{cc} corresponding to the cyan region decreased the allowed region which with future lattice calculations could be decreased further. Comparing the blue and cyan regions we note that the reduction in the error on η_{ct} would be welcomed as well. It should also be stressed that in a given CMFV model with fixed $S(v)$ the uncertainties are reduced further. This is illustrated with the black range for the case of the SM. Finally an impact on Fig. 7 will have a precise measurement of γ or equivalently precise lattice determination of ξ . We illustrate this impact in Fig. 8 by setting in the plots of Fig. 7 $\gamma = (67 \pm 1)^\circ$.

5 Going Beyond CMFV

It is evident from our analysis and in particular from Fig. 4 that in the likely case in which the central values of $|V_{cb}|$, $F_{B_s} \sqrt{\hat{B}_{B_s}}$ and $F_{B_d} \sqrt{\hat{B}_{B_d}}$ will only change by a few percent but their uncertainties will be significantly reduced, one will have to look beyond the CMFV framework to understand the $\Delta F = 2$ data. Models like Littlest Higgs model with T-parity, various Randall-Sundrum scenarios and general supersymmetric models having many free parameters will be able to remove all these tensions although improved precision on the quantities in question would imply new constraints on the parameters of these models. Here we mention simpler models where the discussion can be made

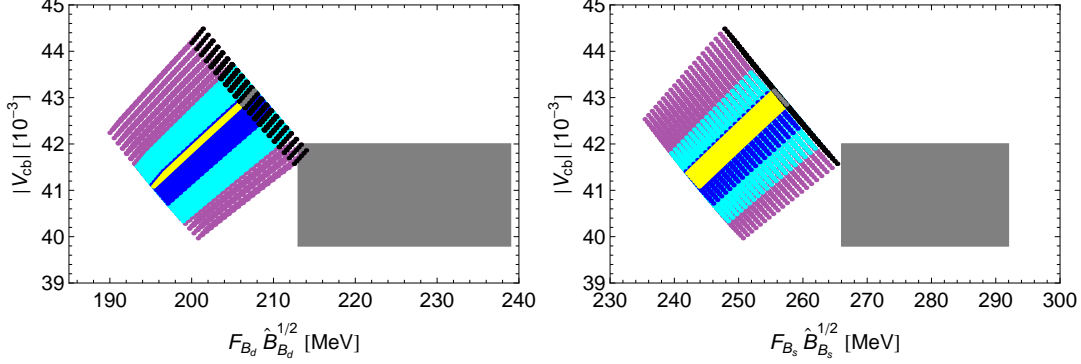


Figure 8: $|V_{cb}|$ versus $F_{B_d} \sqrt{\hat{B}_{B_d}}$ and $F_{B_s} \sqrt{\hat{B}_{B_s}}$ as in Fig. 7 but for $\gamma = (67 \pm 1)^\circ$.

more transparent than in those more complicated models.

First in the case of MFV at large [64–66] in which new operators can contribute the situation looks a bit better. Here the presence of left-right scalar operators in a 2HDM or the MSSM naturally interferes destructively with the SM contribution suppressing in particular ΔM_s [67], but only slightly ΔM_d and having no impact on ε_K . Even if in these models charged Higgs and SUSY particles can enhance $S(v)$ one can expect that still values of $|V_{cb}|$ will be required to be above the ones quoted in Table 1 and the ones of $F_{B_s} \sqrt{\hat{B}_{B_s}}$ and $F_{B_d} \sqrt{\hat{B}_{B_d}}$ have to be suppressed. But the problem will be softer than in CMFV. On the other hand left-right operators affect the ratio $\Delta M_s / \Delta M_d$ which in CMFV models agrees well with data. The solution then would be left-left scalar operators which affect ΔM_s and ΔM_d by the same factor and keep this ratio fixed.

The latter solution appears to be the best for the 2HDM with flavour blind phases, the so-called 2HDM_{MFV} [68, 69] as well. But here the presence of new CP-violating phases changes the situation radically as now $|V_{ub}|$ can be chosen larger in order to fit ε_K . The enhanced value of $\sin 2\beta$ can be suppressed through these new phases. This implies on the other hand enhancement of the asymmetry $S_{\psi\phi}$ to values $0.15 - 0.20$ [11] which is 2σ above the central experimental value from LHCb and could be ruled out when the data improve.

Possibly the simplest solution to the problems of various models with MFV is to reduce the flavour symmetry $U(3)^3$ to $U(2)^3$ [70–76]. As pointed out in [26] in this case NP effects in ε_K and $B_{s,d}^0 - \bar{B}_{s,d}^0$ are not correlated with each other so that the enhancement of ε_K and suppression of $\Delta M_{s,d}$ can be achieved if necessary in principle for the values of $|V_{cb}|$, $F_{B_s} \sqrt{\hat{B}_{B_s}}$ and $F_{B_d} \sqrt{\hat{B}_{B_d}}$ in Table 1.

In particular,

- NP effects in ε_K are of CMFV type and ε_K can only be enhanced but the size of necessary enhancement depends on the value of $|V_{ub}|$ which similar to 2HDM_{MFV} does not have to be low.

- In $B_{s,d}^0 - \bar{B}_{s,d}^0$ system, the ratio $\Delta M_s/\Delta M_d$ is equal to the one in the SM and in good agreement with the data. But in view of new CP-violating phases φ_{B_d} and φ_{B_s} even in the presence of only SM operators, $\Delta M_{s,d}$ can be suppressed. But the $U(2)^3$ symmetry implies $\varphi_{B_d} = \varphi_{B_s}$ and consequently a triple $S_{\psi K_S} - S_{\psi\phi} - |V_{ub}|$ correlation which constitutes an important test of this NP scenario [26].
- The important advantage of $U(2)^3$ models over $2\text{HDM}_{\overline{\text{MFV}}}$ is that in the case of $S_{\psi\phi}$ being very small or even having opposite sign to SM prediction, this framework can survive with concrete prediction for $|V_{ub}|$.

6 Conclusions

In this paper we have determined $F_{B_s}\sqrt{\hat{B}_{B_s}}$, $F_{B_d}\sqrt{\hat{B}_{B_d}}$, $|V_{cb}|$, $|V_{ub}|$, $|V_{td}|$ and $|V_{ts}|$, necessary to fit very precise data on ε_K , ΔM_d , ΔM_s and $S_{\psi K_S}$ in CMFV models as functions of the phase γ and the sole NP free parameter in the $\Delta F = 2$ transitions, the value of the box diagram function $S(v)$. An important ingredient of this analysis was a very small error on \hat{B}_K from lattice and the fact that \hat{B}_K comes within 1 – 2% from its large N value 0.75. The results are shown in Table 2 and Figs. 3-5. The chart showing the execution of our strategy can be found in Fig. 1.

Our main messages from this analysis are as follows:

- The tension between ε_K and $\Delta M_{s,d}$ in CMFV models accompanied with $|\varepsilon_K|$ being smaller than the data within the SM, cannot be removed by varying $S(v)$ when the present input parameters in Table 1 are used.
- Rather the value of $|V_{cb}|$ has to be increased and the values of $F_{B_s}\sqrt{\hat{B}_{B_s}}$ and $F_{B_d}\sqrt{\hat{B}_{B_d}}$ decreased relatively to the presently quoted lattice values. These enhancements and suppressions are correlated with each other and depend on γ . The allowed regions in the space of these three parameters, the most important results of our paper, are shown in Figs. 4, 7 and 8.
- The knowledge of long distance contributions to ΔM_K accompanied by the very precise experimental value of the latter allows a significant reduction of the present uncertainty in the value of the QCD factor η_{cc} under the plausible assumption that ΔM_K in CMFV models is fully dominated by the SM contribution. This implies the reduction of the theoretical error in ε_K and in turn the reduction of the error in the extraction of the favoured value of $|V_{cb}|$ in the CMFV framework. Present estimates of these long distance contributions using large N QCD allow for an optimism but more sophisticated lattice calculations are required to fully execute this idea.

We have also discussed simplest extensions of the SM which could in principle offer a better description of the data in case CMFV would fail to do so. Models with $U(2)^3$ flavour symmetry appear to us as most efficient in this respect while being still very simple. In order to see whether the CMFV framework will survive final tests from $\Delta F = 2$ transitions further progress from lattice calculations and experimental measurements is required. Our wish list includes:

- In particular improved lattice calculations of $F_{B_s}\sqrt{\hat{B}_{B_s}}$, $F_{B_d}\sqrt{\hat{B}_{B_d}}$ and ξ but also of \hat{B}_K , \hat{B}_{B_s} and \hat{B}_{B_d} .
- Calculation of long distance contribution to ΔM_K in order to reduce the error on η_{cc} as proposed by us.
- Improved experimental data on $|V_{cb}|$, $|V_{ub}|$, γ , $S_{\psi K_S}$ and $S_{\psi\phi}$. In particular a measurement of $S_{\psi\phi}$ significantly different from 0.04 would signal the presence of new phases beyond the CMFV framework.

The correlations identified in this paper will allow to monitor the future developments, likely to indicate that new sources of flavour and CP-violation beyond the CMFV framework are present in nature. In this context our main message is the following one. While until now the search for NP through rare decays did not bring any convincing signs of its presence, it could turn out soon that $\Delta F = 2$ transitions combined with the progress made by lattice community will herald the appearance of particular type of NP. This would not only be exciting news but would also give some directions for searching for this NP in rare decays and even high-energy processes.

Acknowledgements

We thank Jean-Marc Gérard for many illuminating comments and Chris Sachrajda for useful information on the progress in lattice calculations. This research was fully financed and done in the context of the ERC Advanced Grant project “FLAVOUR” (267104).

References

- [1] A. J. Buras, P. Gambino, M. Gorbahn, S. Jager, and L. Silvestrini, *Universal unitarity triangle and physics beyond the standard model*, *Phys. Lett.* **B500** (2001) 161–167, [[hep-ph/0007085](#)].
- [2] A. J. Buras, *Minimal flavor violation*, *Acta Phys. Polon.* **B34** (2003) 5615–5668, [[hep-ph/0310208](#)].
- [3] M. Blanke, A. J. Buras, D. Guadagnoli, and C. Tarantino, *Minimal Flavour Violation Waiting for Precise Measurements of ΔM_s , $S_{\psi\phi}$, A_{SL}^s , $|V_{ub}|$, γ and $B_{s,d}^0 \rightarrow \mu^+\mu^-$* , *JHEP* **10** (2006) 003, [[hep-ph/0604057](#)].

-
- [4] M. Blanke and A. J. Buras, *Lower bounds on $\Delta M_{s,d}$ from constrained minimal flavour violation*, *JHEP* **0705** (2007) 061, [[hep-ph/0610037](#)].
- [5] E. Lunghi and A. Soni, *Possible Indications of New Physics in B_d -mixing and in $\sin(2\beta)$ Determinations*, *Phys. Lett.* **B666** (2008) 162–165, [[arXiv:0803.4340](#)].
- [6] A. J. Buras and D. Guadagnoli, *Correlations among new CP violating effects in $\Delta F = 2$ observables*, *Phys. Rev.* **D78** (2008) 033005, [[arXiv:0805.3887](#)].
- [7] **UTfit Collaboration** Collaboration, M. Bona *et. al.*, *An Improved Standard Model Prediction Of $BR(B \rightarrow \tau\nu)$ And Its Implications For New Physics*, *Phys.Lett.* **B687** (2010) 61–69, [[arXiv:0908.3470](#)].
- [8] A. Lenz, U. Nierste, J. Charles, S. Descotes-Genon, A. Jantsch, *et. al.*, *Anatomy of New Physics in $B - \bar{B}$ mixing*, *Phys.Rev.* **D83** (2011) 036004, [[arXiv:1008.1593](#)].
- [9] E. Lunghi and A. Soni, *Possible evidence for the breakdown of the CKM-paradigm of CP-violation*, *Phys.Lett.* **B697** (2011) 323–328, [[arXiv:1010.6069](#)].
- [10] A. J. Buras, M. V. Carlucci, L. Merlo, and E. Stamou, *Phenomenology of a Gauged $SU(3)^3$ Flavour Model*, [arXiv:1112.4477](#).
- [11] A. J. Buras and J. Girrbach, *BSM models facing the recent LHCb data: A First look*, *Acta Phys.Polon.* **B43** (2012) 1427, [[arXiv:1204.5064](#)].
- [12] C. Davies, *Standard Model Heavy Flavor physics on the Lattice*, *PoS LATTICE2011* (2011) 019, [[arXiv:1203.3862](#)].
- [13] E. Gámiz, *Flavour physics from lattice QCD*, [arXiv:1303.3971](#).
- [14] Y. Aoki, R. Arthur, T. Blum, P. Boyle, D. Brommel, *et. al.*, *Continuum Limit of B_K from 2+1 Flavor Domain Wall QCD*, *Phys.Rev.* **D84** (2011) 014503, [[arXiv:1012.4178](#)].
- [15] T. Bae, Y.-C. Jang, C. Jung, H.-J. Kim, J. Kim, *et. al.*, *B_K using HYP-smeared staggered fermions in $N_f = 2 + 1$ unquenched QCD*, *Phys.Rev.* **D82** (2010) 114509, [[arXiv:1008.5179](#)].
- [16] **ETM Collaboration** Collaboration, M. Constantinou *et. al.*, *B_K -parameter from $N_f = 2$ twisted mass lattice QCD*, *Phys.Rev.* **D83** (2011) 014505, [[arXiv:1009.5606](#)].
- [17] G. Colangelo, S. Durr, A. Juttner, L. Lellouch, H. Leutwyler, *et. al.*, *Review of lattice results concerning low energy particle physics*, *Eur.Phys.J.* **C71** (2011) 1695, [[arXiv:1011.4408](#)].

-
- [18] J. A. Bailey, T. Bae, Y.-C. Jang, H. Jeong, C. Jung, *et. al.*, *Beyond the Standard Model corrections to $K^0 - \bar{K}^0$ mixing*, *PoS LATTICE2012* (2012) 107, [arXiv:1211.1101].
- [19] S. Durr, Z. Fodor, C. Hoelbling, S. Katz, S. Krieg, *et. al.*, *Precision computation of the kaon bag parameter*, *Phys.Lett.* **B705** (2011) 477–481, [arXiv:1106.3230].
- [20] J. Laiho, E. Lunghi, and R. S. Van de Water, *Lattice QCD inputs to the CKM unitarity triangle analysis*, *Phys. Rev.* **D81** (2010) 034503, [arXiv:0910.2928]. Updates available on <http://latticeaverages.org/>.
- [21] B. D. Gaiser, T. Tsao, and M. B. Wise, *Parameters of the six quark model*, *Annals Phys.* **132** (1981) 66.
- [22] A. J. Buras and J.-M. Gérard, *1/N Expansion for Kaons*, *Nucl.Phys.* **B264** (1986) 371.
- [23] W. A. Bardeen, A. J. Buras, and J.-M. Gérard, *The B Parameter Beyond the Leading Order of 1/N Expansion*, *Phys.Lett.* **B211** (1988) 343.
- [24] J.-M. Gérard, *An upper bound on the Kaon B-parameter and $\text{Re}(\epsilon_K)$* , *JHEP* **1102** (2011) 075, [arXiv:1012.2026].
- [25] **UTfit Collaboration** Collaboration, M. Bona *et. al.*, *Model-independent constraints on $\Delta F=2$ operators and the scale of new physics*, *JHEP* **0803** (2008) 049, [arXiv:0707.0636]. Updates available on <http://www.utfit.org>.
- [26] A. J. Buras and J. Girrbach, *On the Correlations between Flavour Observables in Minimal $U(2)^3$ Models*, *JHEP* **1301** (2013) 007, [arXiv:1206.3878].
- [27] A. J. Buras, F. De Fazio, J. Girrbach, and M. V. Carlucci, *The Anatomy of Quark Flavour Observables in 331 Models in the Flavour Precision Era*, *JHEP* **1302** (2013) 023, [arXiv:1211.1237].
- [28] A. J. Buras, F. De Fazio, and J. Girrbach, *The Anatomy of Z' and Z with Flavour Changing Neutral Currents in the Flavour Precision Era*, *JHEP* **1302** (2013) 116, [arXiv:1211.1896].
- [29] A. J. Buras, J. Girrbach, and R. Ziegler, *Particle-Antiparticle Mixing, CP Violation and Rare K and B Decays in a Minimal Theory of Fermion Masses*, arXiv:1301.5498.
- [30] A. J. Buras, R. Fleischer, J. Girrbach, and R. Knegjens, *Probing New Physics with the $B_s \rightarrow \mu^+ \mu^-$ Time-Dependent Rate*, arXiv:1303.3820.
- [31] A. J. Buras, F. De Fazio, J. Girrbach, R. Knegjens, and M. Nagai, *The Anatomy of Neutral Scalars with FCNCs in the Flavour Precision Era*, arXiv:1303.3723.

-
- [32] S. H. Kettell, L. Landsberg, and H. H. Nguyen, *Alternative technique for standard model estimation of the rare kaon decay branchings $BR(K \rightarrow \pi\nu\bar{\nu})$ (SM)*, *Phys.Atom.Nucl.* **67** (2004) 1398–1407, [[hep-ph/0212321](#)].
- [33] A. J. Buras, F. Parodi, and A. Stocchi, *The CKM matrix and the unitarity triangle: Another look*, *JHEP* **0301** (2003) 029, [[hep-ph/0207101](#)].
- [34] A. J. Buras, D. Guadagnoli, and G. Isidori, *On ϵ_K beyond lowest order in the Operator Product Expansion*, *Phys.Lett.* **B688** (2010) 309–313, [[arXiv:1002.3612](#)].
- [35] M. Blanke, A. J. Buras, K. Gemmler, and T. Heidsieck, *$\Delta F = 2$ observables and $B \rightarrow X_q\gamma$ in the Left-Right Asymmetric Model: Higgs particles striking back*, *JHEP* **1203** (2012) 024, [[arXiv:1111.5014](#)].
- [36] R. Dowdall, C. Davies, R. Horgan, C. Monahan, and J. Shigemitsu, *B-meson decay constants from improved lattice NRQCD and physical u, d, s and c sea quarks*, [arXiv:1302.2644](#).
- [37] **Particle Data Group** Collaboration, K. Nakamura *et. al.*, *Review of particle physics*, *J.Phys.G* **G37** (2010) 075021.
- [38] **Particle Data Group** Collaboration, J. Beringer *et. al.*, *Review of Particle Physics (RPP)*, *Phys.Rev.* **D86** (2012) 010001.
- [39] K. Chetyrkin, J. Kuhn, A. Maier, P. Maierhofer, P. Marquard, *et. al.*, *Charm and Bottom Quark Masses: An Update*, *Phys.Rev.* **D80** (2009) 074010, [[arXiv:0907.2110](#)].
- [40] **HPQCD Collaboration** Collaboration, I. Allison *et. al.*, *High-Precision Charm-Quark Mass from Current-Current Correlators in Lattice and Continuum QCD*, *Phys.Rev.* **D78** (2008) 054513, [[arXiv:0805.2999](#)].
- [41] A. J. Buras, M. Jamin, and P. H. Weisz, *Leading and next-to-leading QCD corrections to ϵ parameter and $B^0 - \bar{B}^0$ mixing in the presence of a heavy top quark*, *Nucl. Phys.* **B347** (1990) 491–536.
- [42] J. Urban, F. Krauss, U. Jentschura, and G. Soff, *Next-to-leading order QCD corrections for the $B^0 - \bar{B}^0$ mixing with an extended Higgs sector*, *Nucl. Phys.* **B523** (1998) 40–58, [[hep-ph/9710245](#)].
- [43] **CDF Collaboration**, **D0 Collaboration** Collaboration, T. Aaltonen *et. al.*, *Combination of the top-quark mass measurements from the Tevatron collider*, *Phys.Rev.* **D86** (2012) 092003, [[arXiv:1207.1069](#)].
- [44] **Heavy Flavor Averaging Group** Collaboration, Y. Amhis *et. al.*, *Averages of B-Hadron, C-Hadron, and tau-lepton properties as of early 2012*, [arXiv:1207.1158](#).

-
- [45] **LHCb collaboration** Collaboration, R. Aaij *et. al.*, *Measurement of CP violation and the B_s^0 meson decay width difference with $B_s^0 \rightarrow J/\psi K^+ K^-$ and $B_s^0 \rightarrow J/\psi \pi^+ \pi^-$ decays*, [arXiv:1304.2600](#).
 - [46] **LHCb Collaboration** Collaboration, G. Raven, *Measurement of the CP violation phase ϕ_s in the B_s system at LHCb*, [arXiv:1212.4140](#).
 - [47] J. Brod and M. Gorbahn, *Next-to-Next-to-Leading-Order Charm-Quark Contribution to the CP Violation Parameter ε_K and ΔM_K* , *Phys.Rev.Lett.* **108** (2012) 121801, [[arXiv:1108.2036](#)].
 - [48] J. Brod and M. Gorbahn, *ε_K at Next-to-Next-to-Leading Order: The Charm-Top-Quark Contribution*, *Phys.Rev.* **D82** (2010) 094026, [[arXiv:1007.0684](#)].
 - [49] C. Tarantino, *Flavor Lattice QCD in the Precision Era*, [arXiv:1210.0474](#).
 - [50] R. Fleischer and R. Knegjens, *In Pursuit of New Physics with $B_s^0 \rightarrow K^+ K^-$* , *Eur.Phys.J.* **C71** (2011) 1532, [[arXiv:1011.1096](#)].
 - [51] G. 't Hooft, *A Planar Diagram Theory for Strong Interactions*, *Nucl.Phys.* **B72** (1974) 461.
 - [52] G. 't Hooft, *A Two-Dimensional Model for Mesons*, *Nucl.Phys.* **B75** (1974) 461.
 - [53] E. Witten, *Baryons in the $1/n$ Expansion*, *Nucl.Phys.* **B160** (1979) 57.
 - [54] W. A. Bardeen, A. J. Buras, and J.-M. Gérard, *The $\Delta I = 1/2$ Rule in the Large N Limit*, *Phys.Lett.* **B180** (1986) 133.
 - [55] W. A. Bardeen, A. J. Buras, and J.-M. Gérard, *The $K \rightarrow \pi\pi$ Decays in the Large N Limit: Quark Evolution*, *Nucl.Phys.* **B293** (1987) 787.
 - [56] W. A. Bardeen, A. J. Buras, and J.-M. Gérard, *A Consistent Analysis of the $\Delta I = 1/2$ Rule for K Decays*, *Phys.Lett.* **B192** (1987) 138.
 - [57] T. Blum, P. Boyle, N. Christ, N. Garron, E. Goode, *et. al.*, *Lattice determination of the $K \rightarrow (\pi\pi)_{I=2}$ Decay Amplitude A_2* , [arXiv:1206.5142](#).
 - [58] **RBC Collaboration, UKQCD Collaboration** Collaboration, P. Boyle *et. al.*, *Emerging understanding of the $\Delta I = 1/2$ Rule from Lattice QCD*, [arXiv:1212.1474](#).
 - [59] J. Bijnens, J.-M. Gérard, and G. Klein, *The $K_L - K_S$ mass difference*, *Phys.Lett.* **B257** (1991) 191–195.
 - [60] J.-M. Gérard, *Electroweak interactions of hadrons*, *Acta Phys.Polon.* **B21** (1990) 257–305.

- [61] J. F. Donoghue, E. Golowich, and B. R. Holstein, *Long Distance chiral contributions to $K_L - K_S$ mass difference*, *Phys.Lett.* **B135** (1984) 481.
- [62] J.-M. Gérard, C. Smith, and S. Trine, *Radiative kaon decays and the penguin contribution to the $\Delta I = 1/2$ rule*, *Nucl.Phys.* **B730** (2005) 1–36, [[hep-ph/0508189](#)].
- [63] N. Christ, T. Izubuchi, C. Sachrajda, A. Soni, and J. Yu, *Long distance contribution to the $K_L - K_S$ mass difference*, [arXiv:1212.5931](#).
- [64] R. S. Chivukula and H. Georgi, *Composite technicolor standard model*, *Phys. Lett.* **B188** (1987) 99.
- [65] L. J. Hall and L. Randall, *Weak scale effective supersymmetry*, *Phys. Rev. Lett.* **65** (1990) 2939–2942.
- [66] G. D’Ambrosio, G. F. Giudice, G. Isidori, and A. Strumia, *Minimal flavour violation: An effective field theory approach*, *Nucl. Phys.* **B645** (2002) 155–187, [[hep-ph/0207036](#)].
- [67] A. J. Buras, P. H. Chankowski, J. Rosiek, and L. Slawianowska, *Correlation between δm_s and $b_{d,s}^0 \rightarrow \mu^+ \mu^-$ in supersymmetry at large $\tan \beta$* , *Phys. Lett.* **B546** (2002) 96–107, [[hep-ph/0207241](#)].
- [68] A. J. Buras, M. V. Carlucci, S. Gori, and G. Isidori, *Higgs-mediated FCNCs: Natural Flavour Conservation vs. Minimal Flavour Violation*, *JHEP* **1010** (2010) 009, [[arXiv:1005.5310](#)].
- [69] A. J. Buras, G. Isidori, and P. Paradisi, *EDMs versus CPV in $B_{s,d}$ mixing in two Higgs doublet models with MFV*, *Phys.Lett.* **B694** (2011) 402–409, [[arXiv:1007.5291](#)].
- [70] R. Barbieri, G. Isidori, J. Jones-Perez, P. Lodone, and D. M. Straub, *$U(2)$ and Minimal Flavour Violation in Supersymmetry*, *Eur.Phys.J.* **C71** (2011) 1725, [[arXiv:1105.2296](#)].
- [71] R. Barbieri, P. Campli, G. Isidori, F. Sala, and D. M. Straub, *B -decay CP -asymmetries in SUSY with a $U(2)^3$ flavour symmetry*, *Eur.Phys.J.* **C71** (2011) 1812, [[arXiv:1108.5125](#)].
- [72] R. Barbieri, D. Buttazzo, F. Sala, and D. M. Straub, *Flavour physics from an approximate $U(2)^3$ symmetry*, *JHEP* **1207** (2012) 181, [[arXiv:1203.4218](#)].
- [73] R. Barbieri, D. Buttazzo, F. Sala, and D. M. Straub, *Less Minimal Flavour Violation*, *JHEP* **1210** (2012) 040, [[arXiv:1206.1327](#)].
- [74] A. Crivellin, L. Hofer, and U. Nierste, *The MSSM with a Softly Broken $U(2)^3$ Flavor Symmetry*, *PoS EPS-HEP2011* (2011) 145, [[arXiv:1111.0246](#)].

-
- [75] A. Crivellin, L. Hofer, U. Nierste, and D. Scherer, *Phenomenological consequences of radiative flavor violation in the MSSM*, *Phys.Rev.* **D84** (2011) 035030, [[arXiv:1105.2818](#)].
- [76] A. Crivellin and U. Nierste, *Supersymmetric renormalisation of the CKM matrix and new constraints on the squark mass matrices*, *Phys.Rev.* **D79** (2009) 035018, [[arXiv:0810.1613](#)].